

# A time frequency analysis of wave packet fractional revivals

**Suranjana Ghosh and J Banerji**

Theoretical Physics Division

Physical Research Laboratory, Navrangpura, Ahmedabad 380 009, India

E-mail: [sanjana@prl.res.in](mailto:sanjana@prl.res.in), [jay@prl.res.in](mailto:jay@prl.res.in)

**Abstract.** We show that the time frequency analysis of the autocorrelation function is, in many ways, a more appropriate tool to resolve fractional revivals of a wave packet than the usual time domain analysis. This advantage is crucial in reconstructing the initial state of the wave packet when its coherent structure is short-lived and decays before it is fully revived. Our calculations are based on the model example of fractional revivals in a Rydberg wave packet of circular states. We end by providing an analytical investigation which fully agrees with our numerical observations on the utility of time-frequency analysis in the study of wave packet fractional revivals.

(Figures in this article are in colour only in the electronic version)

## 1. Introduction

In certain quantum systems with nonlinear energy spectra, a suitably prepared wave packet will, in the course of its evolution, regain its initial form periodically. This is known as the revival of the wave packet. At some intermediate times, the evolving wave packet will break up into a set of replicas of its original form. This is known as the fractional revivals of the wave packet [1, 2]. It has been shown that the phenomena of revival and fractional revival occur in the wave packet dynamics of various atomic, molecular and optical systems such as Rydberg atoms [3, 4, 5, 6, 7, 8, 9, 10, 11], optical parametric oscillators [12, 13, 14], the Jaynes-Cummings model [15, 16, 17], transient signals from multilevel quantum systems [18], potential wells [19, 20, 21, 22] and molecular vibrational states [23, 24, 25, 26]. Extensions to systems for which the energy spectrum depends on two quantum numbers, have also been made in recent years [27, 28, 29, 30, 31, 32]. These phenomena have been experimentally observed in both atomic [6, 9, 10, 11] and molecular systems [25].

A widely used method for probing the revival dynamics of wave packets is based on a study of the autocorrelation function [4, 24, 33]. This method is directly related to the observable signal in the pump-probe type experiments for studying the wave packet dynamics. The autocorrelation function for an evolving wave packet  $\Psi(r, t)$  is given by the overlap integral  $A(t) = \langle \Psi(r, t) | \Psi(r, 0) \rangle$ .

The auto-correlation function is a time series whose Fourier Transform (FT) will reveal all the frequencies, but will be unable to provide any information on when a particular frequency appears. This is important in the present context as the frequencies are time-varying. In other words, fractional revivals of a particular order occurs at particular instants of time. What is really desirable is a time-frequency analysis of the auto-correlation function such that we not only know all the frequencies, but also get information on when a particular frequency occurs. This is the objective of the present work.

For the purpose of time-frequency analysis, short-time Fourier transform (STFT) has often been used in the literature. This method divides the whole time series in several windows, each of certain fixed width. Then the FT is performed in each window for obtaining the frequency information. Unfortunately, the time-frequency information obtained by this method has not always been satisfactory as its fixed window length does compromise on the frequency resolution. The method of continuous wavelet transform (CWT) [34, 35, 36, 37, 38, 39, 40] overcomes the preset resolution problem of STFT by using a variable length window. This transform, by design provides good localisation in both time and frequency. The subject area of wavelets, developed mostly over the last fifteen years, is at the forefront of much current research in pure and applied mathematics, physics, computer science and engineering. This transform has emerged over recent years as a powerful time-frequency analysis. A narrow window is used for the analysis of the high frequencies and gives a better time resolution. A wider window is used for the analysis of low frequencies and gives a better frequency resolution. The continuous wavelet transform (CWT) of a signal  $f(t)$  is defined as

$$T(s, \tau) = \frac{1}{\sqrt{s}} \int f(t) \phi^* \left( \frac{t - \tau}{s} \right) dt \quad (1)$$

This transformed signal is a function of two variables,  $s$  and  $\tau$  that are used respectively to scale and translate the wavelet window whereas  $\phi^*$  is the complex conjugate of the

transforming function known as the mother wavelet for the CWT. In our study we have used the Morlet wavelet as the mother wavelet. The contribution to the signal energy at the specific scale  $s$  and location  $\tau$  is given by the two dimensional wavelet energy density function known as the scalogram:

$$E(s, \tau) = |T(s, \tau)|^2. \quad (2)$$

The frequencies are inversely proportional to the scale parameter, and thus  $s$  and  $\tau$  together help provide information in the time-frequency plane. In this paper, we present a case study to show that a wavelet based time-frequency analysis is superior in many ways to the standard time-domain analysis of the auto-correlation function.

## 2. Fractional Revivals of a Rydberg wave packet

We consider a Rydberg wave packet which is a superposition of circular Hydrogenic states having  $l = m = n - 1$  [5]. The time dependent wave function for a localized wave packet formed as a one dimensional superposition of eigenstates may be written as

$$\psi(\vec{r}, t) = \sum_n c_n \psi_n(\vec{r}) e^{-iE_n t} \quad (3)$$

As a pre-requisite for obtaining fractional revivals, we assume that the weighting probabilities  $|c_n|^2$  are strongly peaked around a mean value  $\bar{n}$  with a spread  $\Delta n = n_{\max} - n_{\min} \ll \bar{n}$ . This allows us to expand the energy eigenvalues  $E_n = -(2n^2)^{-1}$  (in atomic unit) in a Taylor series in  $n$  as follows.

$$E_n = E_{\bar{n}} + E'_{\bar{n}}(n - \bar{n}) + \frac{1}{2}E''_{\bar{n}}(n - \bar{n})^2 + \frac{1}{6}E'''_{\bar{n}}(n - \bar{n})^3 + \dots \quad (4)$$

Neglecting the overall time dependent phase and considering up to the second order term, we may write  $E_n$  as

$$E_n = 2\pi \left\{ \frac{(n - \bar{n})}{T_{\text{cl}}} + \frac{(n - \bar{n})^2}{T_{\text{rev}}} \right\}, \quad (5)$$

where each term in the expansion defines important characteristic time scale that depend on  $\bar{n}$  ;

$$T_{\text{cl}} = \frac{2\pi}{|E'_{\bar{n}}|}, \quad T_{\text{rev}} = \frac{2\pi}{\frac{1}{2}|E''_{\bar{n}}|}. \quad (6)$$

Since the energy spectrum is known in this case, one obtains

$$T_{\text{cl}} = 2\pi\bar{n}^3, \quad T_{\text{rev}} = 2T_{\text{cl}}\bar{n}/3. \quad (7)$$

The absolute square of autocorrelation function is

$$f(t) = |A(t)|^2 = \sum_{n,m} |c_n|^2 |c_m|^2 e^{-iE_{nm}t/\hbar}, \quad (8)$$

where  $E_{nm} = E_n - E_m$ .

Fig. 1(a) shows a plot of  $|A(t)|^2$  as a function of time. This plot was generated by choosing  $|c_n|^2$  as a Gaussian distribution with  $\bar{n} = 320$ ,  $\Delta n = 40$  and a FWHM given by  $\sigma = 2.5$ .

Peaks appearing in Fig. 1 (a), are the signature of revivals and fractional revivals. Fast Fourier transform (FFT) of this time series data gives the individual spectral components in the frequency plane as shown in Fig. 1 (b). Although we can get

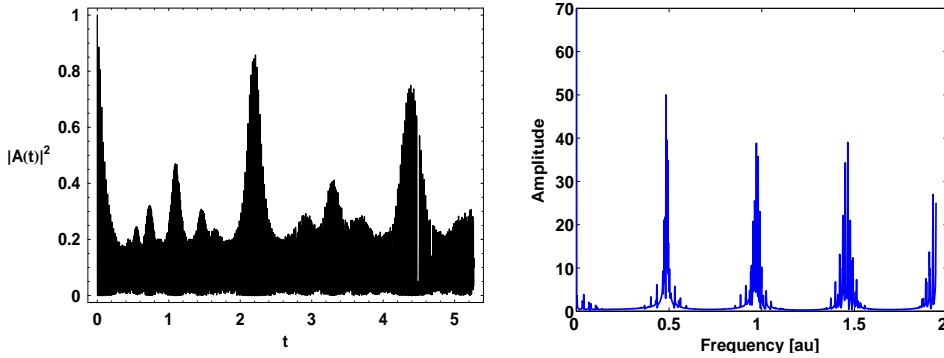


**Figure 1:** (a) Autocorrelation function of a Rydberg wave packet with  $\bar{n} = 320$ ,  $\Delta n = 40$  and  $\sigma = 2.5$ . Time  $t$  is in a.u. (in the unit of  $10^{10}$ ). (b) Spectral components present in the autocorrelation function of the Rydberg wave packet. Frequency is in a.u. (in the unit of  $10^{-8}$ ).

complete frequency information in this way, we do not have any idea on which frequency appears at what time. On the other hand, the autocorrelation time series can be recovered by using the inverse FFT, but the frequency information goes away completely.

Our goal is to acquire some frequency information in some particular times of interest. In the next section, we make use of continuous wavelet transform to investigate how one is able to resolve time and frequency in a better way.

### 3. Time-Frequency Analysis

Wavelet based time-frequency representation or scalogram of the time series data  $f(t) = |A(t)|^2$  is shown in Fig. 2. The scalogram was computed by using the *Time-Frequency Tool Box (TFTB) for MatLab* [41]. Here, we have used the Morlet wavelet, described as a complex exponential modulated by a Gaussian envelope. It is a function of time and given by  $\varphi(t) = \pi^{-1/4} e^{i\omega_0 t} e^{-t^2/2}$ , with the central frequency  $\omega_0$ . Let  $\Delta t$  and  $\Delta\omega$  be the RMS duration and bandwidth respectively of the mother wavelet  $\varphi(t)$ , where  $\Delta t$  is given by

$$\Delta t \equiv \sqrt{\frac{\int_{-\infty}^{\infty} (t - t_0)^2 |\varphi(t)|^2 dt}{\int_{-\infty}^{\infty} |\varphi(t)|^2 dt}}, \quad (9)$$

The term inside the square root is the second moment of the wavelet centered at  $t_0$ . Similarly the bandwidth of the wavelet is

$$\Delta\omega \equiv \sqrt{\frac{\int_{-\infty}^{\infty} (\omega - \omega_0)^2 |\varphi(\omega)|^2 d\omega}{\int_{-\infty}^{\infty} |\varphi(\omega)|^2 d\omega}}. \quad (10)$$

This mother wavelet is then used to build a set of daughter wavelets by translating  $\varphi(t)$  in time, and by dilating or contracting  $\varphi(t)$ , which not only adjusts the mean frequency but also the spread of the daughter wavelet.

Consider the case, when the mother wavelet is scaled by  $s$ . The Fourier transform of  $\varphi(t/s)$  is  $|s|\varphi(s\omega)$ . The RMS duration becomes  $\Delta t(s) = |s|\Delta t$  and the corresponding

RMS bandwidth is  $\Delta\omega(s) = \Delta\omega/s$ . It implies  $\Delta t(s)\Delta\omega(s) = \Delta t\Delta\omega$ , which is independent of the scaling parameter  $s$ . Also, the RMS bandwidth is not affected by the translation parameter  $\tau$  because translating a function does not affect the magnitude of its FT. For our chosen mother wavelet  $\varphi(t)$ , Eqs. (9) and (10) yield  $\Delta t = \Delta\omega = 1/\sqrt{2}$  so that  $\Delta\omega\Delta t = 1/2$ , which is independent of scaling and translation. Thus the uncertainty of time localisation is accompanied by an increase in the uncertainty of frequency localisation or vice versa.

Referring to Fig. 2, we note that several patches appear in a rectangular array on the time-frequency plane. Each patch is centered about a particular frequency and a particular time. To help us understand the occurrence of these patches, we undertake an analytical approach as described below. Recall that the absolute square of the autocorrelation function is given by Eq. (8). Writing  $y = (t - \tau)/s$ , the CWT of  $f(t)$  can be written as

$$T(\tau, s) = \sqrt{s} \int_{-\infty}^{\infty} f(y s + \tau) \phi^*(y) dy. \quad (11)$$

where  $\phi(y)$  is the Morlet with shifted time  $\tau$  and scaled by  $s$ :

$$\phi(y) = \pi^{-1/4} e^{i\omega_0 y} e^{-y^2/2}. \quad (12)$$

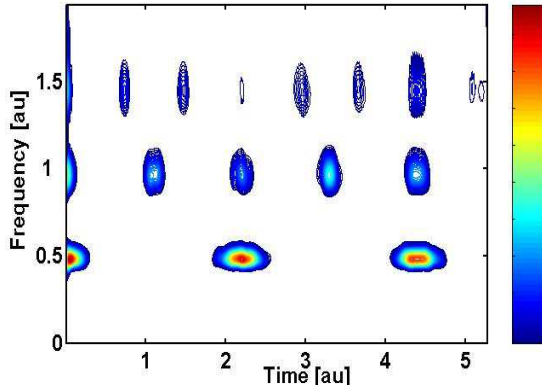


**Figure 2:** Time-frequency representation of the autocorrelation function of Rydberg atom. Time  $t$  (in the unit of  $10^{10}$ ) and frequency (in the unit of  $10^{-8}$ ) are in a.u.

Substituting in Eq. (11) and performing the integration over  $y$ , we get

$$T(\tau, s) = \sqrt{2\pi s} \sum_{n,m} |c_n|^2 |c_m|^2 \pi^{-1/4} e^{-iE_{nm}\tau/\hbar} e^{-(\omega_0 + sE_{nm}/\hbar)^2/2}. \quad (13)$$

Maximum values of  $T(\tau, s)$ , corresponding to a particular scale parameter  $s$  should occur whenever the factor  $e^{-(\omega_0 + sE_{nm}/\hbar)^2/2}$  approaches unity. This gives rise to a constraint:

$$\omega_0 = -sE_{nm}/\hbar. \quad (14)$$

Since the distribution functions  $|c_n|^2$  and  $|c_m|^2$  are peaked about  $\bar{n}$ , the central frequency of each frequency band in Fig. 1(b) can be obtained by setting  $n = \bar{n}$  and  $m = \bar{n} + p$ , where  $p$  is an integer. Since  $\omega_0$  is positive, we must insist that  $p$  is a

positive integer. Substituting in Eq. (14) and using the quadratic approximation (5) for the energy eigenvalues, we immediately get

$$\omega_0 = \frac{2\pi sp}{T_{\text{cl}}} \left( 1 - p \frac{T_{\text{cl}}}{T_{\text{rev}}} \right) \quad (15)$$

Since the scale parameter  $s$  is related to frequency  $f$  by the relation  $s = \omega_0/(2\pi f)$  and  $T_{\text{cl}} \ll T_{\text{rev}}$ , we finally obtain the simple formulae

$$f_p = \frac{p}{T_{\text{cl}}}, \quad s = \frac{\omega_0}{2\pi f_p}. \quad (16)$$

The above formula correctly predicts the central frequencies around which the spectral components are clustered in the frequency plane as was shown earlier in Fig. 1(b). Note that each horizontal band in Fig. 2 has a spread about its central frequency. We will now show that the terms corresponding to these frequencies add up coherently in the expression for  $T(\tau, s)$  at a particular time  $\tau$  given by

$$\tau = \frac{k}{2p} T_{\text{rev}} \quad (17)$$

where  $k$  is an integer.

Coherent addition of terms would require that the phase factor  $\exp(-iE_{nm}\tau/\hbar)$  be the same for these terms. That is, for arbitrary values of  $n$  and  $n'$ , one should be able to satisfy the condition

$$\tau E_{n,n+p} = \tau E_{n',n'+p} + 2\pi N \quad (18)$$

where  $N$  is an integer number. Using the approximation (5), it is now easy to show that  $\tau$  is indeed given by the expression (17). An equivalent and simpler way of deriving this result is to insist that the phase factor  $\exp(-i\tau E_{n,n+p})$  is independent of  $n$ .

The expression (17) gives us the time instants at which  $|A(t)|^2$  is peaked. Specifically, it tells us which frequency beats occur at what times. The lowest frequency beats  $f_1$  occur for  $p = 1$  at times  $t/T_{\text{rev}} = 1/2, 1, 3/2, 2, \dots$ . Similarly, the frequency beats  $f_2$  corresponding to  $p = 2$ , occur at  $t/T_{\text{rev}} = 1/4, 1/2, 3/4, 1, \dots$ . Thus the patches appearing in the bottom row give the transition frequency between any two consecutive levels ( $p = 1$ ), the ones on the next row are the transition frequencies corresponding to  $p = 2$  and so on. In this way, frequency bands, depicted in Fig. 2, trace out the signature of fractional revivals.

Thus interestingly, in time-frequency plane, one can find both time and frequency information from the two time scales  $T_{\text{cl}}$  and  $T_{\text{rev}}$  by using the expressions (17) and (16). In fact, these two expressions provide the location of each patch in the time-frequency plane. As an example, let us consider the fourth maximum or patch in the third harmonic appearing in Fig. 2. Here, the third harmonic corresponds to  $p = 3$ , so the frequency information corresponding to this patch can be obtained from Eq. (16), which is  $f_3 = 1.457 \times 10^{-8}$  a.u., as shown in Fig. 2. The corresponding value for time can be obtained from Eq. (17). In this case,  $k = 4$ , and  $p = 3$ , so the patch will appear at  $t = \frac{2}{3} T_{\text{rev}}$ .

#### 4. Advantages of the Time-Frequency Representation

It is seen that the wavelet based time-frequency representation provides localisation in both time and frequency. Higher order fractional revivals and their localisation in

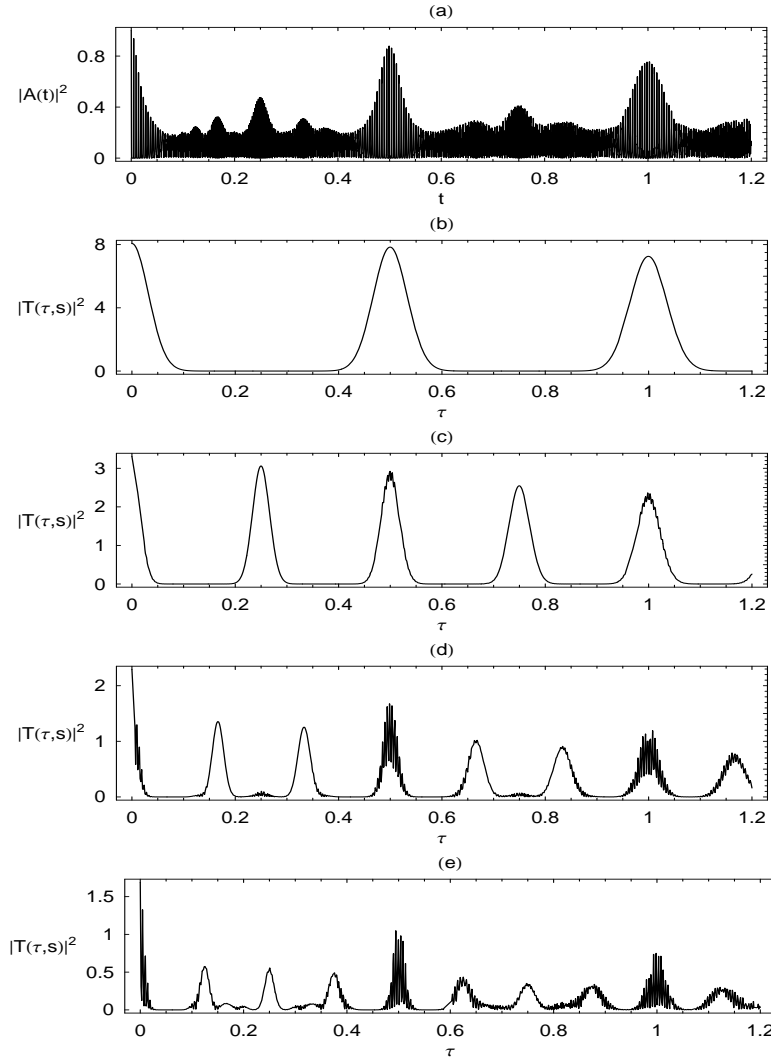


**Figure 3:** (a) Autocorrelation function of Rydberg atomic system with  $\sigma = 2.5$ , (b), (c), (d) and (e) show  $|T(\tau, s)|^2$  for  $s = 1.96, 0.97, 0.65$  and  $0.48$  (in unit of  $10^8$ ) respectively. Times are scaled by revival time and  $|T(\tau, s)|^2$  is scaled by  $10^6$ .

time are clearly manifest in the time-frequency plane. We showed how  $T_{\text{rev}}$  and  $T_{\text{cl}}$  are themselves sufficient to explain the time-frequency plane completely.

Note also that the square of the autocorrelation function, plotted as a time series, does not resolve fractional revivals unambiguously. More precisely, the order of the fractional revival cannot always be determined. In contrast, the time frequency representation introduces a parameter  $p$  through Eqs. (16) and (17) that clearly separates out the fractional revivals in a rectangular array on the time-frequency plane. In Fig. 3, we show how the corresponding  $s$  values filter out fractional revivals

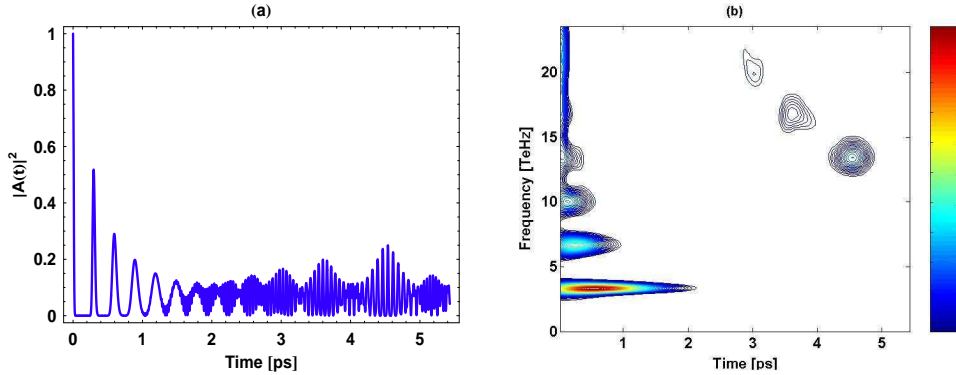


**Figure 4:** (Color online) (a) A short-lived time series of autocorrelation function and (b) its wavelet based time-frequency representation.

from the complicated plot of the autocorrelation function. For  $p = 1$ , one can find  $s$  using Eq. (16). This specific  $s$  value can filter out the signature of fractional revivals as shown in Fig. 3(b). This is also true for the higher order harmonics as shown in Fig. 3(c), (d) and (e) for  $p = 2$ ,  $p = 3$  and  $p = 4$  respectively. These specific values of  $s$ , filter out the signature of the corresponding higher order fractional revivals.

The time-frequency representation can be useful for a wave packet that decays before its revival time. Although the short-time evolution of  $|A(t)|^2$  can still be used to estimate  $T_{cl}$ , no information can be gained about  $T_{rev}$  if the energy spectrum of the system is *not* known. However, as long as the wave packet survives long enough for some patches to occur in the scalogram ( see Fig. 4), one can use Eq. (17) to estimate  $T_{rev}$ . What makes this possible is the better resolution available in the time-frequency plane for the detection of fractional revivals.

## 5. Conclusion

In conclusion, we have made use of the continuous wavelet transform to demonstrate the time-frequency representation of autocorrelation function for the wave packet dynamics of a Rydberg wave packet. An analytical approach is provided to interpret the time-frequency plane and explain our numerical observations. We have shown that the time-frequency representation not only provides a complementary method of analyzing fractional revivals, it is a better tool in resolving fractional revivals. Finally, it is shown that the time-frequency representation may be able to extract information about the revival dynamics of a short-lived system even if the system decays before reaching its revival time.

## Acknowledgments

We thank Dr. P. K. Panigrahi for fruitful discussions and valuable comments.

## References

- [1] Averbukh I Sh and Perelman N F 1989 *Phys. Lett. A* **139** 449-453
- [2] Robinett R W 2004 *Physics Reports* **392** 1-119



- [3] Alber G, Ritsch H and Zoller P 1986 *Phys. Rev. A* **34** 1058-1064
- [4] Nauenberg M 1990 *J. Phys. B: At. Mol. Phys.* **23** L385-L390
- [5] Gaeta Z D and Stroud C R Jr 1990 *Phys. Rev. A* **42** 6308-6313
- [6] Wals *et. al.* 1994 *Phys. Rev. Lett.* **72** 3783-3786
- [7] Bluhm R, Kostelecky V A and Tudose B 1995 *Phys. Rev. A* **52** 2234-2244
- [8] Bluhm R, Kostelecky V A and Tudose B 1996 *Phys. Rev. A* **53** 937-945
- [9] Yeazell J A, Mallalieu M and Stroud C R Jr 1990 *Phys. Rev. Lett.* **64** 2007-2010
- [10] Yeazell J A and Stroud C R Jr 1991 *Phys. Rev. A* **43** 5153-5156
- [11] Meacher D R, Meyler P E, Hughes I G and Ewart P 1991 *J. Phys. B: At. Mol. Phys.* **24** L63-L69
- [12] Drobny G and Jex I 1992 *Phys. Rev. A* **45** 1816-1821
- [13] Jyotsna I V and Agarwal G S 1997 *J. Mod. Opt.* **44** 305-312
- [14] Agarwal G S and Banerji J 1997 *Phys. Rev. A* **55** R4007-R4010
- [15] Eberly J H, Narozhny N B and Sanchez-Mondragon J J 1980 *Phys. Rev. Lett.* **44** 1323-1326
- [16] Rempe G, Walther H and Klein N 1987 *Phys. Rev. Lett.* **58** 353-356
- [17] Knight P L and Shore B W 1993 *Phys. Rev. A* **48** 642-655
- [18] Leichtle C, Averbukh I Sh and Schleich W P 1996 *Phys. Rev. A* **54** 5299-5312
- [19] Aronstein D L and Stroud C 1997 *Phys. Rev. A* **55** 4526-4537
- [20] Grobmann F, Rost J M, and Schleich W P 1997 *J. Phys. A: Math. Gen.* **30** L277-L283
- [21] Shreecharan T, Panigrahi P K and Banerji J 2004 *Phys. Rev. A* **69** 012102-012108
- [22] Roy U, Banerji J and Panigrahi P K 2005 *J. Phys. A: Math. Gen.* **38**, 9115-9125
- [23] Vetchinkin S L and Eryomin V V 1994 *Chem. Phys. Lett.* **222** 394-398
- [24] Eryomin V V, Vetchinkin S I and Umanskii I M 1994 *J. Chem. Phys.* **101**, 10730-10735
- [25] Vrakking M J J, Villeneuve D M and Stolow A 1996 *Phys. Rev. A* **54** R37-R40
- [26] Ghosh S, Chiruvelli A, Banerji J and Panigrahi P K 2006 *Phys. Rev. A* **73** 013411-013414
- [27] Banerji J and Ghosh S 2006 *J. Phys. B: At. Mol. Opt. Phys.* **39** 1113-1123
- [28] Banerji J and Agarwal G S 1999 *Optics Express* **5** 220-229
- [29] Banerji J and Agarwal G S 1999 *Phys. Rev. A* **59** 4777-4783
- [30] Agarwal G S and Banerji J 1998 *Phys. Rev. A* **57** 3880-3884
- [31] Bluhm R, Kostelecky V A and Tudose B 1996 *Phys. Lett. A* **222** 220-226
- [32] Bluhm R, Kostelecky V A and Tudose B 1997 *Phys. Rev. A* **55**, 819-822
- [33] Veilande R and Bersons I 2007 *J. Phys. B: At. Mol. Opt. Phys.* **40** 2111-2119
- [34] Daubechies Ingrid 1992 *Ten Lectures on Wavelets* (SIAM)
- [35] Charles K. Chui 1992 *An Introduction to Wavelets* (ACADEMIC PRESS)
- [36] Polikar R 1999 *The Engineer'S Ultimate Guide to Wavelet Analysis, The Wavelet Tutorial*
- [37] Vela-Arevalo L V and Fox R F 2005 *Phys. Rev. A* **71** 063403-063414
- [38] Lang W C and Forinash K 1998 *Am. J. Phys.* **66** 794-797
- [39] Treviño G and Andreas E L 1999 *Am. J. Phys.* **67** 934-935
- [40] Lang W C and Forinash K 1999 *Am. J. Phys.* **67** 935-936
- [41] Auger F, Flandrin P, Goncalves P and Lemoine O *Time Frequency ToolBox for use with MATLAB*